Cell Reports, Volume *30*

Supplemental Information

Structures of Gα Proteins in Complex with Their Chaperone Reveal Quality Control Mechanisms

Alpay Burak Seven, Daniel Hilger, Makaía M. Papasergi-Scott, Li Zhang, Qianhui Qu, Brian K. Kobilka, Gregory G. Tall, and Georgios Skiniotis

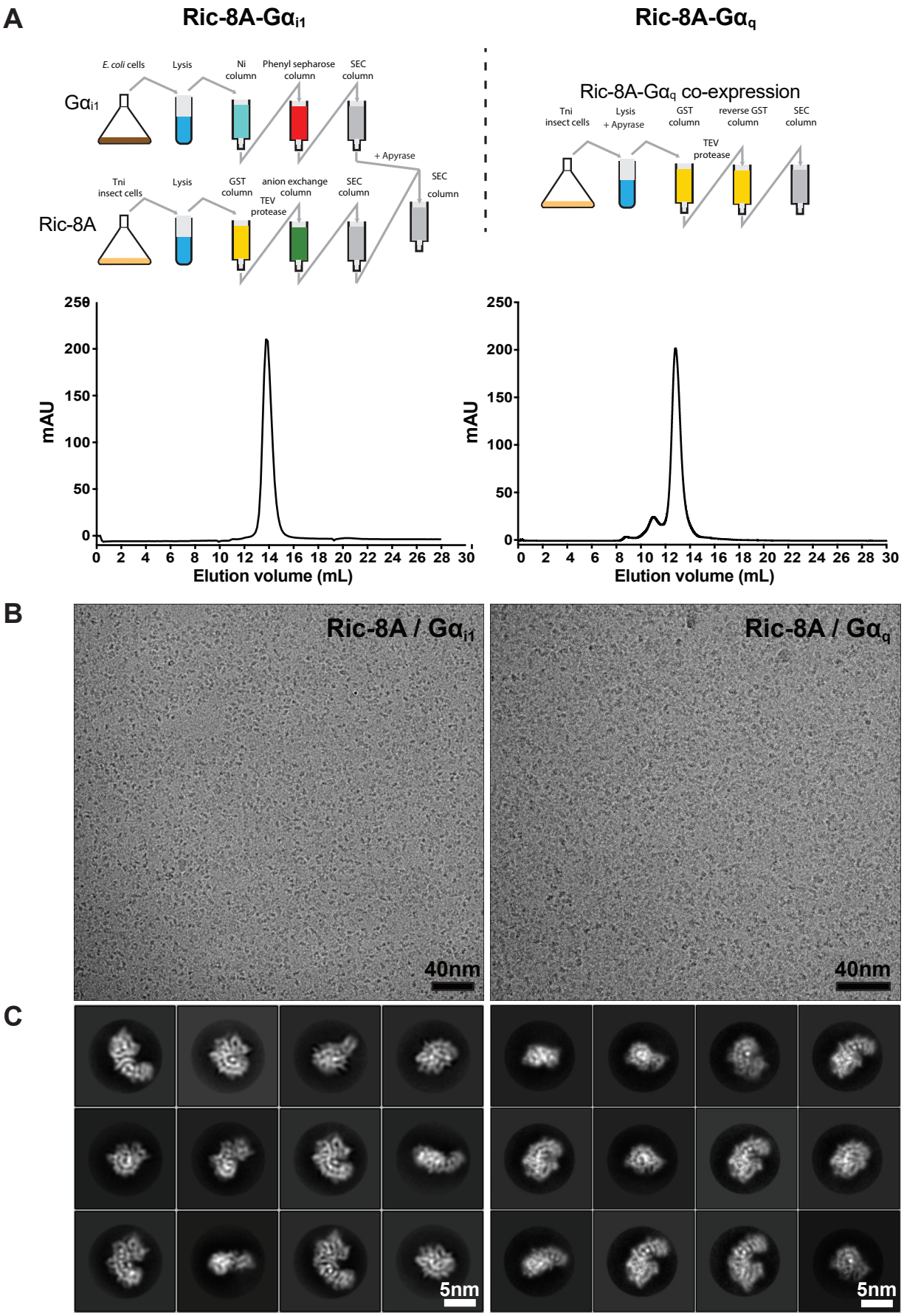

Supplementary Figure 1. Overview of protein purification strategies and cryoEM imaging. (A) Representative elution profile of purified Ric-8A-Gα_{i1} and Ric-8A-Gα_q complexes on Superdex200 Increase 10/300 size-exclusion column. (B) Representative cryoEM micrographs and (C) 2D class averages of full-length Ric-8A bound to full-length Gα_{i1} (left panels) and Gα_q (right panels) for ~200,000 total particle projections with each class representing between 500 to 2500 particle projections. Related to Figure 1.

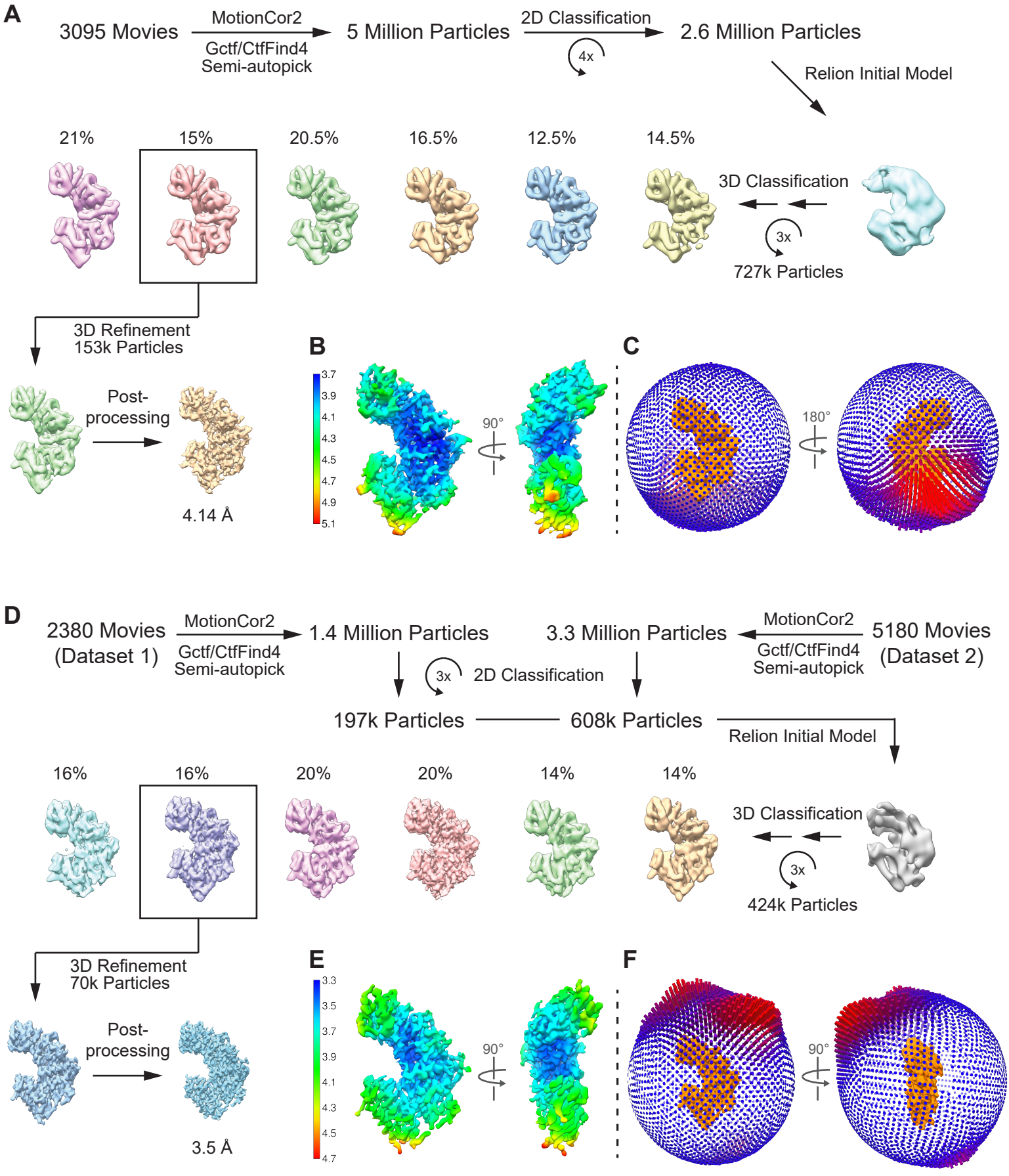

Supplementary Figure 2. CryoEM workflow for the Ric-8A-Gα complexes. (A) CryoEM processing flow-chart, (B) local resolution estimation and (C) angular distribution of the projections contributing to the refined cryoEM map of the Ric-8A-Gα_{i1} complex. (D) CryoEM processing flow-chart, (E) local resolution estimation and (F) angular distribution of the projections contributing to the refined cryoEM map of the Ric-8A-Gα_{q} complex. Related to Figure 1.

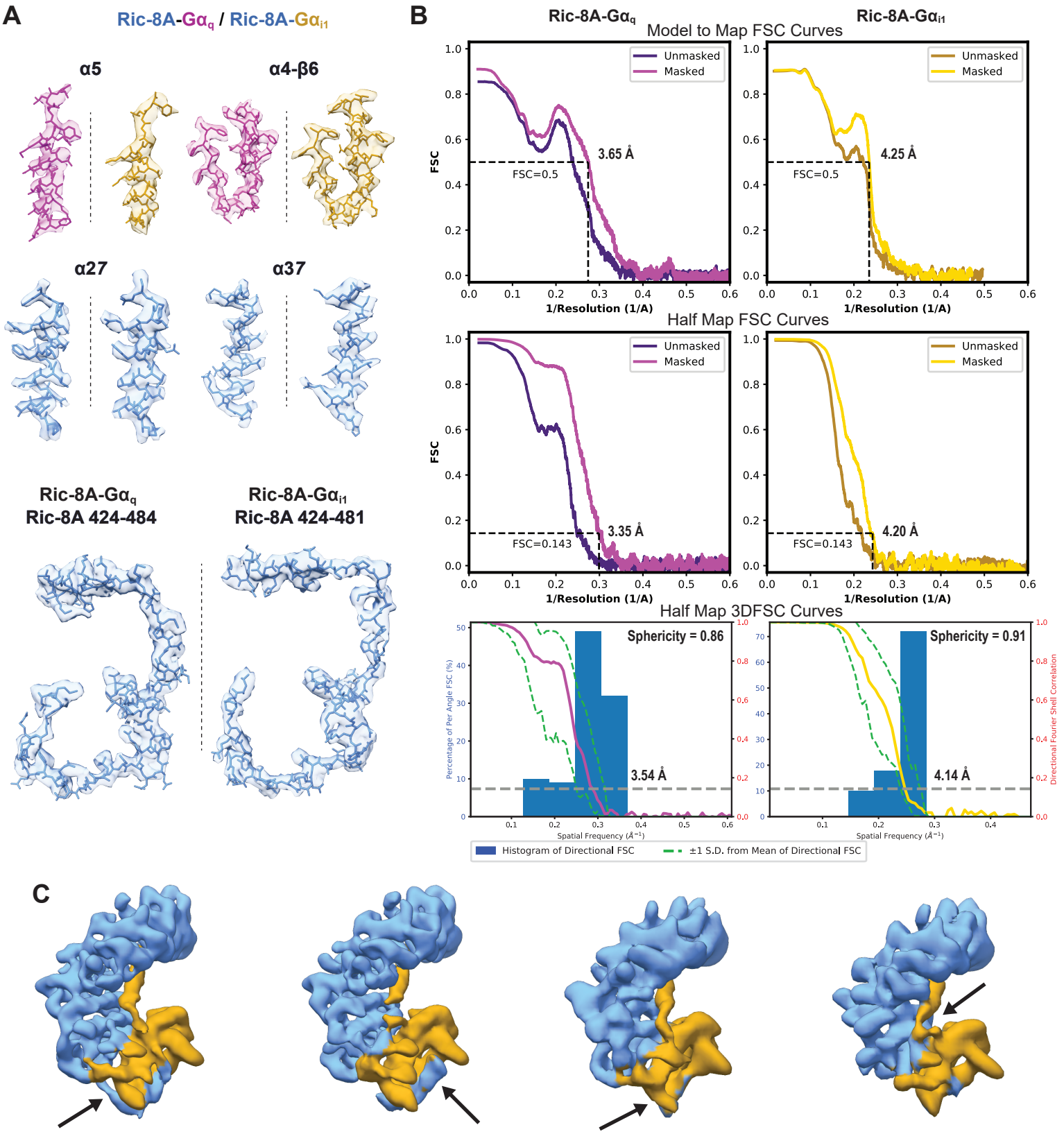

Supplementary Figure 3. CryoEM map quality and validation. (A) Representative cryoEM densities of $G\alpha_q$ (magenta) and $G\alpha_{i1}$ (gold) bound to Ric-8A (blue - left panels for $G\alpha_q$ and right panels for $G\alpha_{i1}$). (B) Fourier shell correlation plots between the model and full map and between the half maps generated using Mtriage in PHENIX and 3DFSC. Dashed lines represent the resolution values at 0.143 FSC for half maps and 0.5 FSC for the model to full map. (D) Structural variability in Ric-8A-Gα complexes. Ric-8A-$G\alpha_{i1}$ particles were subjected to iterative 3D classification rounds followed by refinement to elucidate variation across reconstructions. Corresponding Ric-8A and $G\alpha_{i1}$ densities are colored blue and gold respectively. Four representative classes are shown to highlight the structural variability (indicated by arrows) of the extended C-terminal loop region of Ric-8A, the C-terminal helix of Ric-8A interacting with the switch2 motif of $G\alpha_{i1}$, the Ras-like domain secondary structure elements that interact with guanine nucleotide and the AHD, and the loop between α5 and β6 of $G\alpha_{i1}$ including the TCAT motif respectively. Related to Figure 1.

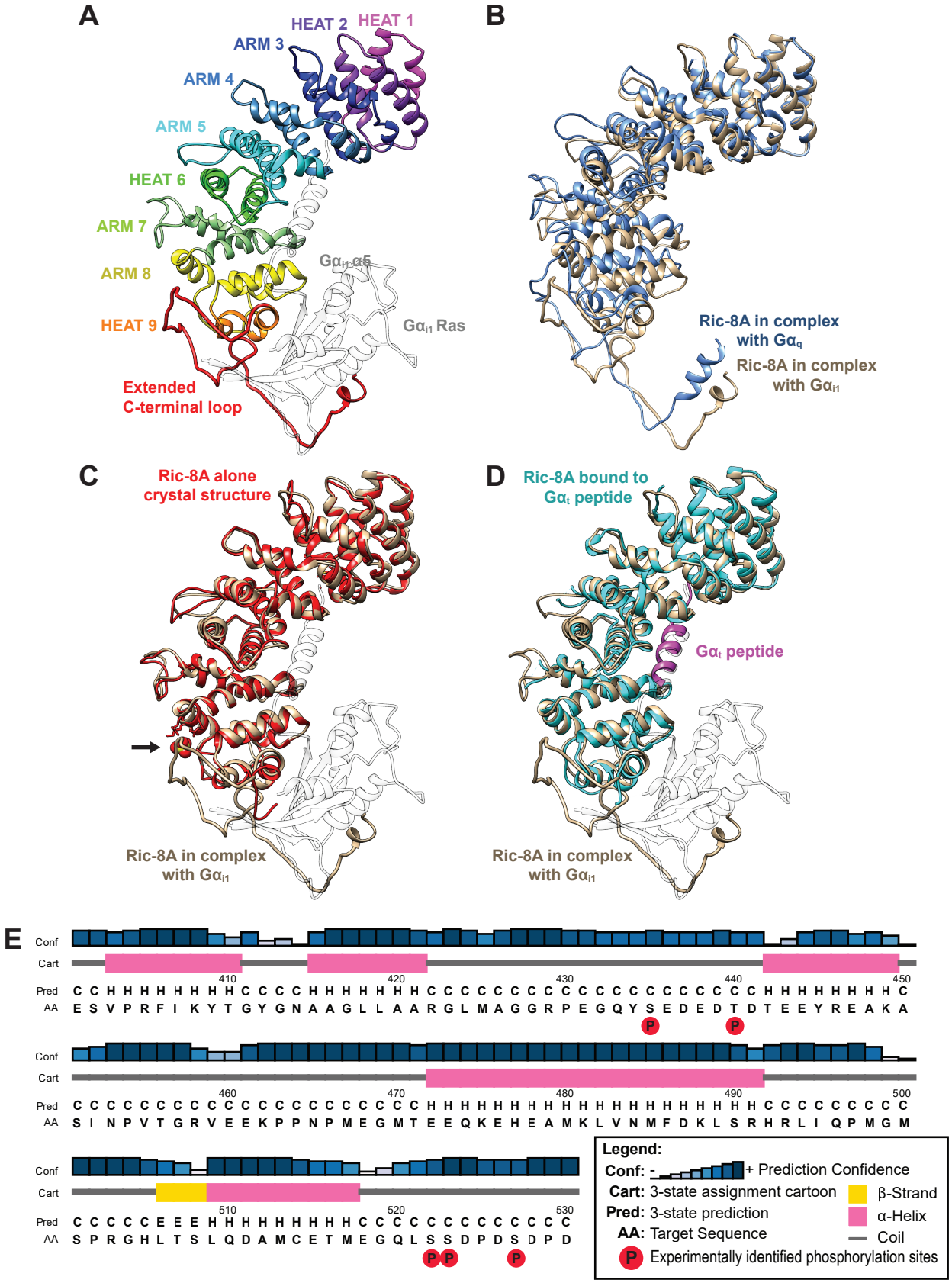

Supplementary Figure 4. Comparison of Ric-8A structures and topology of the C-terminal tail of Ric-8A. (A) Domain architecture of Ric-8A, color coded by ARM/HEAT repeats and the extended C-terminal loop, in complex with $G\alpha_{i1}$ (grey). (B) Comparison of the Ric-8A structures bound to $G\alpha_{i1}$ (tan) and $G\alpha_q$ (blue), aligned according to the first two HEAT repeats of Ric-8A to show the more compact conformation of the core ARM/HEAT repeats of Ric-8A bound to $G\alpha_q$. (C) Ric-8A-$G\alpha_{i1}$ complex structure (tan/grey) compared with the crystal structure of Ric-8A 1-453 alone (red, PDB: 6NMG); the arrow indicates the sulfate ion bound to Ric-8A in the crystal structure. (D) Ric-8A-$G\alpha_{i1}$ complex structure (tan/grey) compared with the crystal structure of Ric-8A (cyan) bound to a Gα transducin ($G\alpha_t$) peptide (purple), (PDB:6N85). (E) Secondary structure prediction of Ric-8A residues 401-530 and experimentaly identified phosphorylation sites. Related to Figure 3.

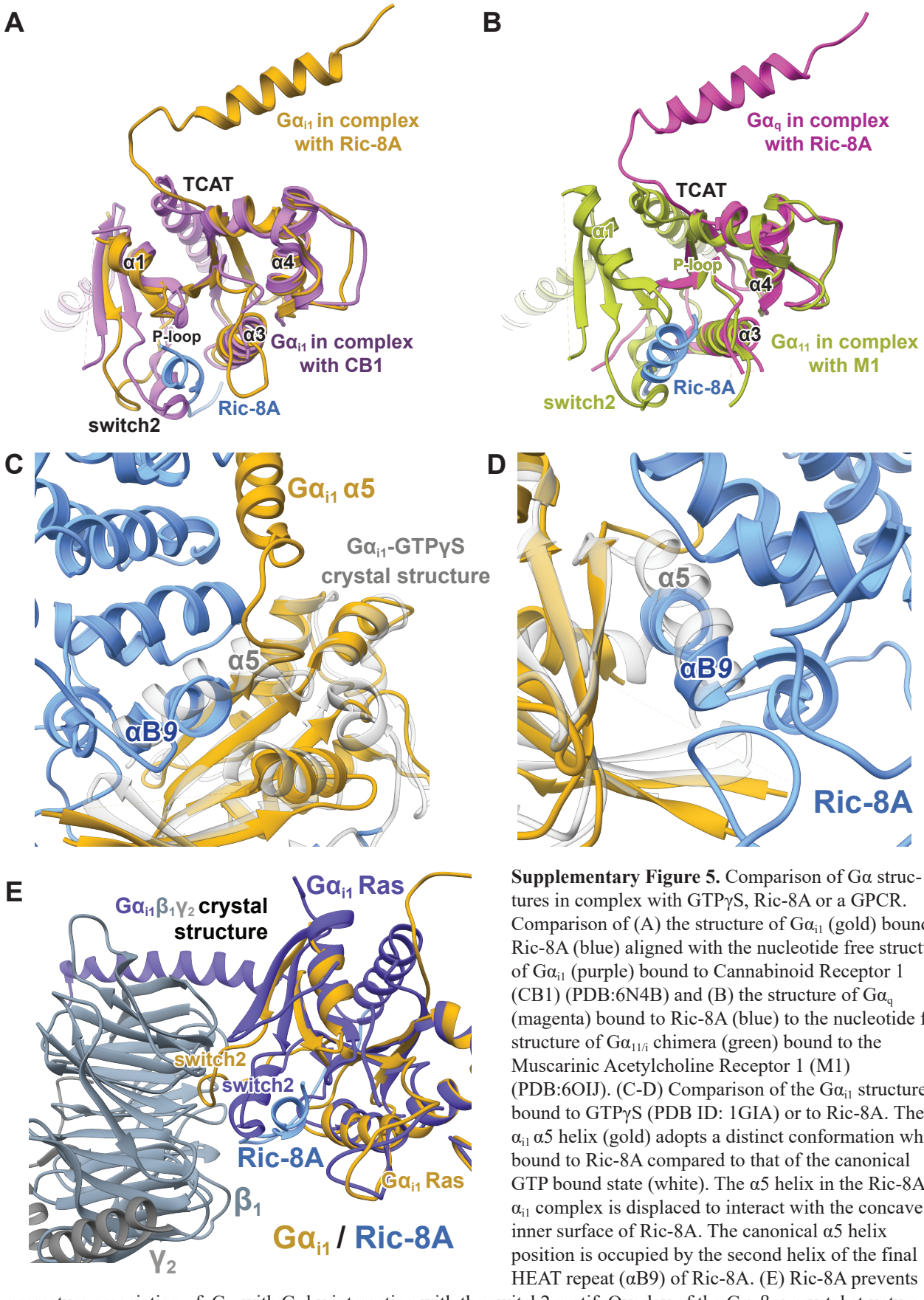

Supplementary Figure 5. Comparison of Gα structures in complex with GTPγS, Ric-8A or a GPCR. Comparison of (A) the structure of $G\alpha_{i1}$ (gold) bound to Ric-8A (blue) aligned with the nucleotide free structure of $G\alpha_{i1}$ (purple) bound to Cannabinoid Receptor 1 (CB1) (PDB:6N4B) and (B) the structure of $G\alpha_{q}$ (magenta) bound to Ric-8A (blue) to the nucleotide free structure of $G\alpha_{11/i}$ chimera (green) bound to the Muscarinic Acetylcholine Receptor 1 (M1) (PDB:6OIJ). (C-D) Comparison of the $G\alpha_{i1}$ structure bound to GTPγS (PDB ID: 1GIA) or to Ric-8A. The G α_{i1} α5 helix (gold) adopts a distinct conformation when bound to Ric-8A compared to that of the canonical GTP bound state (white). The α5 helix in the Ric-8A-G α_{i1} complex is displaced to interact with the concave inner surface of Ric-8A. The canonical α5 helix position is occupied by the second helix of the final HEAT repeat (αB9) of Ric-8A. (E) Ric-8A prevents premature association of $G_{\beta\gamma}$ with G_{α} by interacting with the switch2 motif. Overlay of the $G\alpha_{i1}\beta_1\gamma_2$ crystal structure (PDB ID:1GP2) with the cryoEM model of $G\alpha_{i1}$ (gold) bound to Ric-8A (blue). The switch2 motif interacts with Ric-8A in both $G\alpha_{i1}$ and $G\alpha_{q}$. The switch2 motif of $G\alpha_{i1}$ bound to Ric-8A adopts a different conformation than switch2 motif in either $G\alpha_{i1}$ in complex with $\beta_1\gamma_2$ (slate grey/grey) or $G\alpha_{i1}$ alone. The conformation of Gα switch2 in Ric-8A-Gα structures does not appear to be compatible with canonical $\beta_1\gamma_2$ interaction. Related to Figure 3.

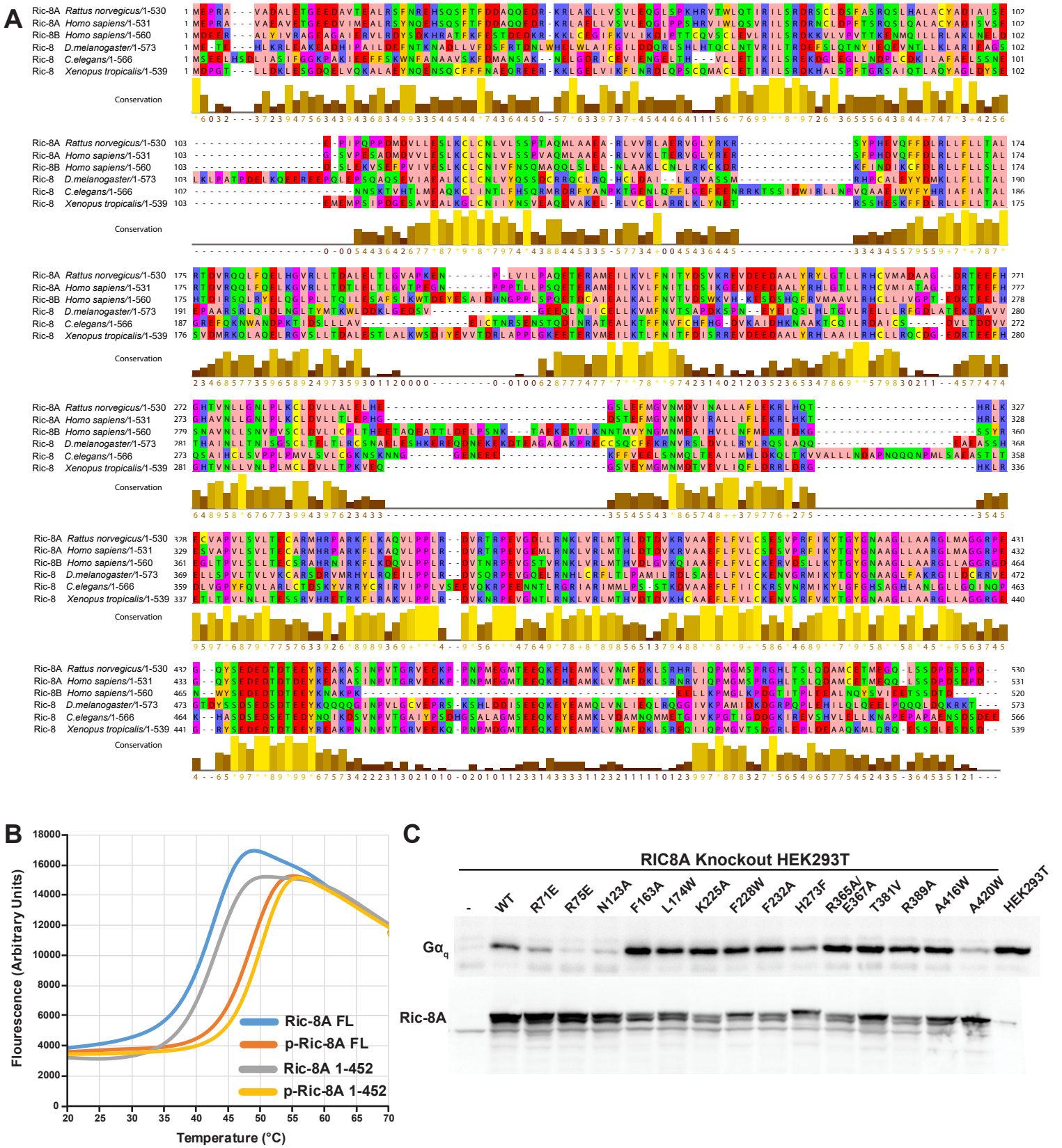

Supplementary Figure 6. Multiple sequence alignment of Ric-8, thermal stability of Ric-8A and expression control of Ric-8A mutants in the cell based Ric-8A complementation assay. (A) The sequence alignment of Ric-8 includes Ric-8A *Rattus norvegicus* (NP_001093990.1), Ric-8A *Homo sapiens*, (NP_001273063.1), Ric-8B *Homo sapiens* (NP_001317074.1), Ric-8 *Drosophila melanogaster* (NP_001285048.1), Ric-8 *Caenorhabditis elegans* (NP_001023561.1) and RIC-8 *Xenopus tropicalis* (NP_989159.1). (B) Thermal stability of full-length Ric-8A (Ric-8A FL), phosphorylated/full-length Ric-8A (p-Ric-8A FL) and truncated Ric-8A (Ric-8A 1-452), and phosphorylated/truncated Ric-8A (p-Ric-8A 1-452). The stability was analyzed using SYPRO Orange fluorescence over increasing temperatures. (C) Knockout of RIC-8A in HEK293T cells results in a $G\alpha_q$ abundance defect (Papasergi-Scott et al., 2018). The rescue of $G\alpha_q$ abundance upon stable expression of Ric-8A mutants was analyzed by quantitative immunoblotting of cell membrane samples. Representative western blot of membrane-bound $G\alpha_q$ is shown in upper panel and Ric-8A in lower panel. Related to Figure 4 and 6.

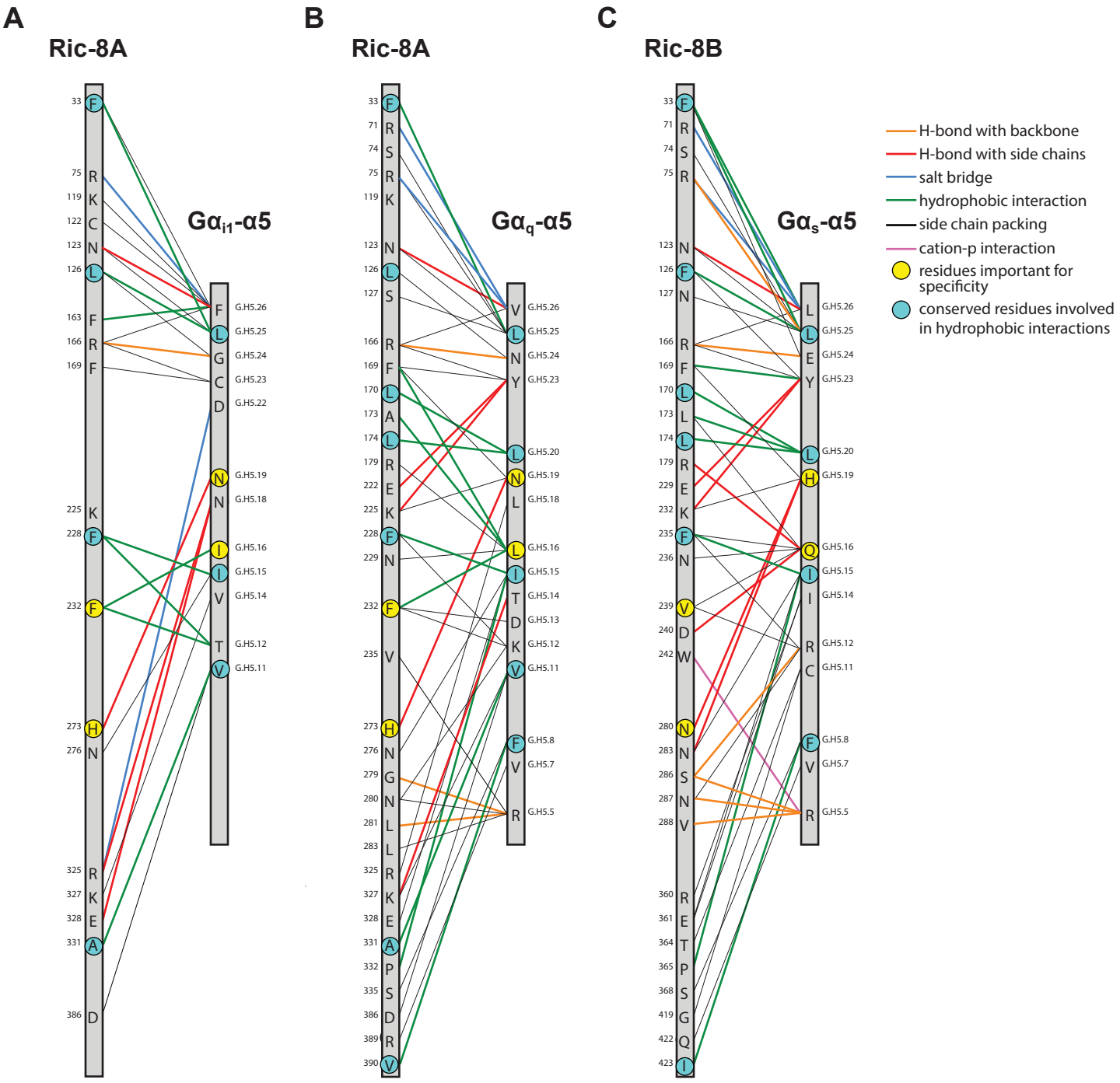

Supplementary Figure 7. Comparison of interaction profiles of the α5 helices with the Ric-8 core domain. Interaction profile of the α5 helix of (A) $G\alpha_{i1}$ or (B) $G\alpha_q$ with Ric-8A identified in the cryoEM structures, and the α5 helix of $G\alpha_s$ with Ric-8B predicted by homology modeling. Residue numbering is based on the "common Gα numbering (CGN) system in superscript" (Flock et al., 2015). Related to Figure 5.

Table S1. CryoEM data collection, refinement and validation statistics. Related to Figure 1.

Data collection and processing	**Ric-8A-Gα$_q$**	**Ric-8A-Gα$_{i1}$**
Magnification	165,000	130,000
Voltage (kV)	300	300
Electron exposure (e$^-$/Å^2)	62	65
Defocus range (μm)	1.0-2.0	1.0-2.0
Pixel size (Å)	0.82	1.06
Symmetry imposed	C1	C1
No. Initial particle images	4,723,551	4,960,082
No. Final particle images	70,439	153,110
Map resolution (Å)	3.5	4.0
FSC threshold	0.143	0.143
Map resolution range (Å)	3.2 – 4.2	3.8-4.5
Map sharpening *B* factor (Å^2)	-90	-180
Refinement		
Initial model used (PDB code)	6NMG (Ric-8A)/3AH8 (Gα$_q$)	6NMG (Ric-8A)/1GP2 (Gα$_{i1}$)
Supplied resolution (Å)	3.5	4.0
FSC threshold	0.5	0.5
Model composition		
Chains	2	2
Non-hydrogen atoms	4,657	5249
Protein residues	603	669
B factors (Å^2)	71.51	142.16
R.m.s. deviations		
Bond lengths (Å)	0.006	0.005
Bond angles (°)	0.934	1.023
Validation		
MolProbity score	1.98	1.97
Clashscore	8.28	7.78
Poor rotamers (%)	0.00	0.00
Ramachandran plot		
Favored (%)	90.53	90.08
Allowed (%)	9.47	9.92
Disallowed (%)	0	0

Table S2. Oligonucleotides. Related to Key Resources Table.

REAGENT or RESOURCE	SOURCE	IDENTIFIER
Oligonucleotides		
$G\alpha_{i1}$-ΔF354_Fw: 5'-AAAGATTGTGGTCTCTAAGC TTCTGAGATCCGGCTGC-3'	Stanford Pan Facility	Custom synthesis
$G\alpha_{i1}$-ΔF354_Rev: 5'-TCTCAGAAGCTTAGAGACCACA ATCTTTTAGATTATTTTTTATGATGACATCTGTTAC-3'	Stanford Pan Facility	Custom synthesis
Quickchange PCR forward primer for R75E: 5'-CCGAATCCTATCCGAAGACCGCAGCTGCC-3'	IDT	Customer synthesis
Quickchange PCR reverse primer for R75E: 5'-GGCAGCTGCGGTCTTCGGATAGGATTCGG-3'	IDT	Customer synthesis
Quickchange PCR forward primer for N123A: 5'-CAAATGCCTGTGTGCTCTTGTGCTCAGCAG-3'	IDT	Customer synthesis
Quickchange PCR reverse primer for N123A: 5'-CTGCTGAGCACAAGAGCACACAGGCATTTG-3'	IDT	Customer synthesis
Quickchange PCR forward primer for F163A: 5'-CGAAGTCCAGTTCGCTGACTTAAGGCTCC-3'	IDT	Customer synthesis
Quickchange PCR reverse primer for F163A: 5'-GGAGCCTTAAGTCAGCGAACTGGACTTCG-3'	IDT	Customer synthesis
Quickchange PCR forward primer for L174W: 5'-CCTGCTAACAGCCTGGCGCACTGATGTGC-3'	IDT	Customer synthesis
Quickchange PCR reverse primer for L174W: 5'-GCACATCAGTGCGCCAGGCTGTTAGCAGG-3'	IDT	Customer synthesis
Quickchange PCR forward primer for K225A: 5'-CATGGAAATCCTCGCAGTGCTCTTTAACATC-3'	IDT	Customer synthesis
Quickchange PCR reverse primer for K225A: 5'-GATGTTAAAGAGCACTGCGAGGATTTCCATG -3'	IDT	Customer synthesis
Quickchange PCR forward primer for F228W: 5'-CCTCAAAGTGCTCTGGAACATCACCTACG-3'	IDT	Customer synthesis
Quickchange PCR reverse primer for F228W: 5'-CGTAGGTGATGTTCCAGAGCACTTTGAGG -3'	IDT	Customer synthesis
Quickchange PCR forward primer for F232A: 5'-CTTTAACATCACCGCCGACTCTGTTAAGAG-3'	IDT	Customer synthesis
Quickchange PCR reverse primer for F232A: 5'-CTCTTAACAGAGTCGGCGGTGATGTTAAAG -3'	IDT	Customer synthesis
Quickchange PCR forward primer for H273F: 5'-GGAGTTCCATGGCTTCACCGTGAATCTCC-3'	IDT	Customer synthesis
Quickchange PCR reverse primer for H273F: 5'-GGAGATTCACGGTGAAGCCATGGAACTCC -3'	IDT	Customer synthesis
Quickchange PCR forward primer for R365A+E367A: 5'-GGGATGTGAGGACTGCGCCTGCGGTGGGGGACCT GCTC-3'	IDT	Customer synthesis
Quickchange PCR reverse primer for R365A+E367A: 5'-GAGCAGGTCCCCCACCGCAGGCGCAGTCCTCACAT CCC -3'	IDT	Customer synthesis
Quickchange PCR forward primer for T381V: 5'-CTTGTCCGCCTCATGGTACACCTGGATACAG-3'	IDT	Customer synthesis
Quickchange PCR reverse primer for T381V: 5'-CTGTATCCAGGTGTACCATGAGGCGGACAAG -3'	IDT	Customer synthesis
Quickchange PCR forward primer for R389A: 5'-GATACAGATGTGAAGGCAGTAGCTGCTGAGTTC-3'	IDT	Customer synthesis
Quickchange PCR reverse primer for R389A: 5'-GAACTCAGCAGCTACTGCCTTCACATCTGTATC -3'	IDT	Customer synthesis

Quickchange PCR forward primer for A416W: 5'-CTACGGGAATGCTTGGGGCCTCCTGGCTG-3'	IDT	Customer synthesis
Quickchange PCR reverse primer for A416W: 5'-CAGCCAGGAGGCCCCAAGCATTCCCGTAG -3'	IDT	Customer synthesis
Quickchange PCR forward primer for A420W: 5'-CTGCTGGCCTCCTGTGGGCCAGGGGCCTCATG -3'	IDT	Customer synthesis
Quickchange PCR reverse primer for A420W: 5'-CATGAGGCCCCTGGCCCACAGGAGGCCAGCAG -3'	IDT	Customer synthesis